

Asteroseismology of the new multiperiodic γ Dor variable HD 239276^{★,★★}

E. Rodríguez¹, V. Costa¹, A.-Y. Zhou², A. Grigahcène³, M. A. Dupret⁴, J. C. Suárez^{1,4,★★★},
A. Moya^{1,4}, M. J. López-González¹, J.-Y. Wei², and Y. Fan²

¹ Instituto de Astrofísica de Andalucía, CSIC, PO Box 3004, 18080 Granada, Spain
e-mail: eloy@iaa.es

² National Astronomical Observatories, Chinese Academy of Sciences, Beijing 100012, PR China

³ CRAAG, Algiers Observatory, BP 63 Bouzareah 16340, Algiers, Algeria

⁴ LESIA, Observatoire de Paris-Meudon, UMR 8109, 92190 Meudon, France

Received 15 March 2006 / Accepted 10 May 2006

ABSTRACT

The variability of HD 239276 was suspected photometrically nearly twenty years ago, but was confirmed with new observations obtained in 2001 during a two-site photometric campaign carried out from Spain, in *uvby* β Strömgren-Crawford photometry, and China, using the Johnson *V* filter. Two low-dispersion spectra were also collected. The results establish this star as a new multiperiodic γ Dor-type pulsator with deficiency in metallicity. Its possible λ Boo nature is discussed. The frequency analysis shows three pulsational frequencies as significant, but some more are probably present among the residuals. The method based on phase shifts and amplitude ratios in multicolour photometry is used to identify the excited modes with non-adiabatic time-dependent convection models. A very good agreement between the theoretical and observed amplitude ratios is obtained and the two main modes are identified as $l = 1$ modes. Nevertheless, our results do not allow us to discriminate between a solar abundance and a metal deficient nature for this star. The frequency ratio method is further used for the identification of the modes. The results suggest low metallicity for this star, but a λ Boo nature may be not ruled out.

Key words. stars: variables: general – stars: individual: HD 239276 – stars: oscillations – techniques: photometric

1. Introduction

The γ Dor-type variables constitute a recently recognized group of main-sequence long-period pulsating stars. They were firstly proposed as a group by Krisciunas (1993) and officially named as γ Dor variables during the meeting on Stellar Pulsation held in Cape Town, in 1995. These stars reside in the zone close to the cool border of the classical instability strip, partially overlapping with the δ Sct-type pulsators. Their relatively long periods, between about 0.3 and 3 days, and small amplitudes, between a few millimagnitudes and some hundredths, are produced by excited nonradial gravity (g) modes of high radial (n) and low angular (l) orders (Handler 1999; Handler & Shobbrook 2002; Henry et al. 2005).

The star HD 239276 (SAO 32177, $V = 9.1$, A3, Simbad 2006) was one of the check stars used for photometric *uvby* β observations on the high amplitude SX Phe star XX Cyg carried out, at the Sierra Nevada Observatory (SNO) (Spain) during July, 1986 and the period June–July, 1987. During these observations a smooth variability was detected in HD 239276, with an amplitude of a few hundredths of magnitude (from peak to peak),

a probable main period longer than 10 h (Fig. 1) and multiperiodic behaviour. Although the calibration of its derived Strömgren-Crawford colour indices (Table 1) places this star much later than A3, and close to the cool border of the δ Sct pulsational region, it is still inside the instability strip (Fig. 2). Binararity as a cause of the variations was discarded because the colour indices were found to vary accordingly with the light curves. These variations probably indicate pulsations. However, the pulsations were in disagreement with the shorter-period δ Sct-type pulsations expected for this star.

Interestingly, at the same time (summer of 1987), similar variations were photometrically detected in the star HR 8799 (=HD 218396) which was proposed as a new member of the γ Dor group by Rodríguez & Zerbi (1995). A more detailed study on HR 8799 was published in Zerbi et al. (1999). Intriguingly, the two stars present very similar photometric characteristics (Table 1 and Fig. 2): their *uvby* β colour indices are very similar as are their locations in the H-R diagram, the two stars are also deficient in metal abundances (the corresponding [Me/H] values are about -0.4). Furthermore, the frequency contents are similar: the main periods are very close to $0^d.5$ ($0^d.51$ in HR 8799, Zerbi et al. 1999; and $0^d.47$ in HD 239276, see below) with both variables showing a multiperiodic behaviour.

Consequently, the 1986–87 observations suggested HD 239276 as a new γ Dor-type variable. In order to confirm this, we undertook a detailed study on its nature and performed a two-site photometric campaign during September–October of 2001 from China and Spain. The results of this investigation

* Tables 2–4 are only available in electronic form at the CDS via anonymous ftp to cdsarc.u-strasbg.fr (130.79.128.5) or via <http://cdsweb.u-strasbg.fr/cgi-bin/qcat?J/A+A/456/261>

** Based on observations collected at Sierra Nevada and Beijing Astronomical observatories.

*** Associate researcher at (4), with financial support from Spanish Consejería de Innovación, Ciencia y Empresa from the Junta de Andalucía local government.

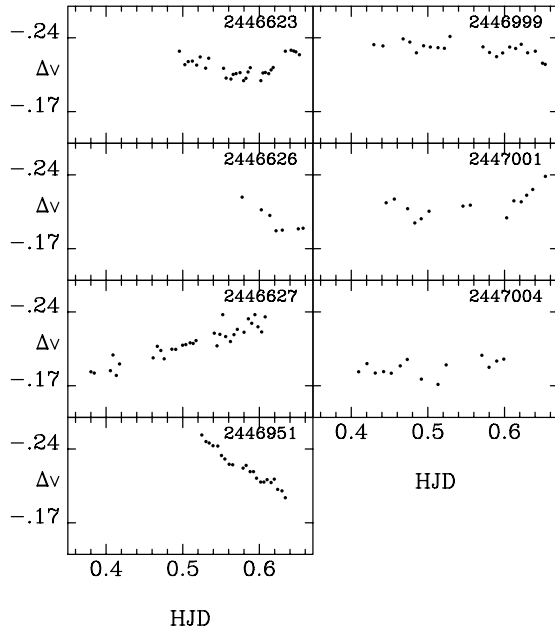


Fig. 1. Observed light variations of HD 239276 in the Strömgren v band during the years 1986 and 1987.

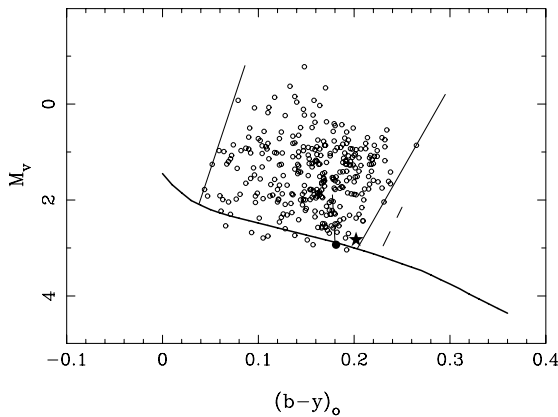


Fig. 2. Location of HD 239276 (star) in the H-R diagram together with HR 8799 (solid circle) and the sample of δ Sct-type pulsators from Rodríguez & Breger (2001). The observational γ Dor edges (dashed lines) are from Handler & Shobbrook (2002).

Table 1. $wby\beta$ indices obtained for HD 239276 during the 1986–87 run and comparison with those available in the bibliography for HR 8799. Sources: 1) present work; 2) Shuster & Nissen (1986); 3) Zerbi et al. (1999).

Star	$b - y$ (mag)	m_1 (mag)	c_1 (mag)	β (mag)	Source
HD 239276	0.201	0.132	0.673	2.730	1
HR 8799	0.188	0.137	0.689	2.742	2
HR 8799	0.181	0.142	0.678	2.745	3

are presented here, including an asteroseismologic study of this new variable.

2. Observations

The observations obtained in China consisted of 3 nights of Johnson V photometry collected with the three-channel high-speed photoelectric photometer P45-A mounted on the

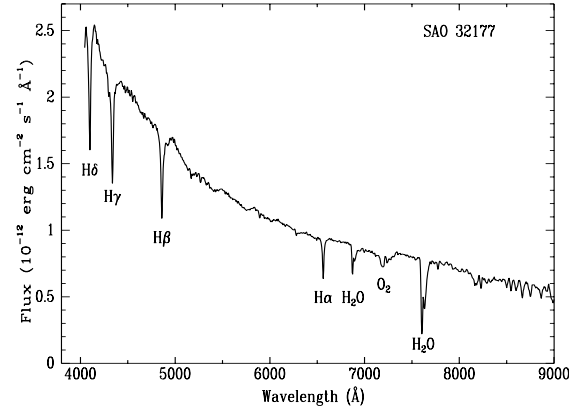


Fig. 3. Spectrum of HD 239276 = SAO 32177.

85-cm Cassegrain telescope at Xinglong Station of the Beijing Astronomical Observatory (BAO). This photometer is commonly used for the Whole Earth Telescope multisite campaigns (WET, Nather et al. 1990) and is equipped with standard Johnson UB V filters and an ST-6 CCD camera for guiding. The exposures were continuous with short integration times of only 5 s for simultaneously measuring sky, variable and one comparison star in the field close to the variable. The data were reduced as magnitude differences relative to the comparison star and averaged every 10 measurements to diminish the noise level.

The observations in Spain consisted of 18 nights of simultaneous observations in the four wby filters of the Strömgren system. The measurements were carried out with the six-channel $wby\beta$ spectrophotometer attached to the 90-cm telescope at SNO (Rodríguez et al. 1997). A few $H\beta$ measurements were also collected for calibration purposes. In these observations, the comparison stars used were C1 = HD 189296 ($V = 6^m 16$, A4V, Simbad 2006), C2 = HD 191096 ($V = 6^m 19$, F4V) and C3 = HD 186760 ($V = 6^m 30$, G0V) with an observational sequence of C1, C2, C3, Var with sky measurements every 2 or 3 cycles. The final data were calculated as magnitude differences of each object relative to C1 and no sign of periodicity was found here for any of the comparison stars.

Besides the photometric observations, two low-dispersion spectra (200 Å/mm) were obtained for the variable using the Cassegrain spectrometer attached to the 2.16 m telescope at BAO (Fig. 3). According to the intensities of $H\beta$, $H\gamma$ and other characteristic lines and their ratio values, the spectrum of HD 239276 is similar to that of an around A9V star. This is later than the A3 listed in the Simbad database (Simbad 2006), but agrees well with F0V, typical of a γ Dor-type variable, as suggested by its colour indices (Tables 1 and 5) and location in the H-R diagram using the calibrations of Gray & Garrison (1989).

3. Photometry

The data, as magnitude differences of variable minus main comparison star versus Heliocentric Julian Date are presented in Tables 2 (wby observations collected in 2001), 3 (Johnson V photometry) and 4 (wby data collected during the 1986–87 run). In the later case, SAO 32139 was the comparison star used. These three tables are available in electronic form at the CDS and can also be requested from the authors. To transform our instrumental data into the standard $wby\beta$ system, we followed the method described in Rodríguez et al. (1997). In the case of the 1986–87 run, a more detailed description is given in Rodríguez et al. (1993).

Table 5. *wby* β indices of HD 239276 and comparison stars obtained during the 2001 run. The pairs below the star names mean the number of points collected for each object in *wby* and β , respectively. The numbers below the magnitudes and colour indices mean the corresponding error bars.

Object	<i>V</i> (mag)	<i>b</i> − <i>y</i> (mag)	<i>m</i> ₁ (mag)	<i>c</i> ₁ (mag)	β (mag)
HD 239276	9.039	0.202	0.137	0.684	2.741
(582, 5)	16	6	5	10	10
C1 = HD 189296	6.090	0.050	0.170	1.054	2.875
(580, 4)					
C2 = HD 191096	6.111	0.277	0.167	0.547	2.673
(571, 4)	3	2	2	4	4
C3 = HD 186760	6.219	0.373	0.185	0.464	2.619
(559, 4)	4	3	2	5	4

Table 6. Reddening and derived physical parameters for HD 239276.

Parameter	Value	Parameter	Value
$E(b - y)$	$0^m000 \pm 0.01$	M_{bol}	$2^m84 \pm 0.3$
$(b - y)_0$	$0^m202 \pm 0.01$	D.M.	$6^m21 \pm 0.3$
m_0	$0^m137 \pm 0.01$	$\log L/L_{\odot}$	0.76 ± 0.12
c_0	$0^m684 \pm 0.01$	T_e (K)	7090 ± 150
δm_1	$0^m046 \pm 0.01$	$\log g$	4.14 ± 0.1
δc_1	$0^m014 \pm 0.02$	Age (Gyr)	1.7 ± 0.1
[Me/H]	-0.40 ± 0.1	M/M_{\odot}	1.42 ± 0.1
M_v	$2^m83 \pm 0.3$	R/R_{\odot}	1.59 ± 0.3

As seen from Tables 1 and 5, the two sets of derived colour indices for the variable are in very good agreement each with each other. Table 5 also lists the indices derived for the comparison stars assuming the values listed for C1 in the homogeneous *wby* β catalogue of Olsen (1996) as the zero point. The error bars listed in this table mean standard deviations of magnitude differences relative to C1. The results obtained for C2 and C3 are in good agreement with those shown in the same catalogue or in that of Hauck & Mermilliod (1998), although there is a discrepancy with respect to the *V* and c_1 values of C3 listed in these catalogues ($V = 6^m299$ and $c_1 = 0^m432$).

In order to estimate the physical parameters of HD 239276 we followed the method described in Rodríguez et al. (2001) using suitable calibrations available in the literature for *wby* β photometry. The results are summarized in Table 6 which place the star well in the γ Dor region as shown in Fig. 2 and slightly deficient in metal content ([Me/H] = -0.40) as mentioned in Sect. 1. The error bars listed in this table are typical taking into account our observational uncertainties in deriving the colour indices and the adopted relations to determine the different parameters. The evolutionary tracks of Claret & Giménez (1995), with $Z = 0.01$, were used to estimate the mass and age of this star. As expected for γ Dor-type variables, HD 239276 is in the main-sequence with a mass of $1.42(\pm 0.1) M_{\odot}$ and age of $1.7(\pm 0.1)$ Gyr as shown in Fig. 4.

However, as discussed in Sect. 1, the photometric characteristics of HD 239276 and HR 8799 are very similar. It is possible that the metal deficiency in HD 239276 is a sign of a λ Boo nature as was already found for HR 8799 by Gray & Kaye (1999). This possibility was also pointed out for the multiperiodic γ Dor star HD 218427 (Rodríguez et al. 2006). Indeed, the three stars are located inside the λ Boo region of both ($m_1, b - y$) and ($[m_1], \beta$) diagrams (Gray 1988; Gray & Corbally 1993). If so, these stars should constitute a small subgroup of metal-poor γ Dor objects similar to the λ Boo stars that are pulsating as

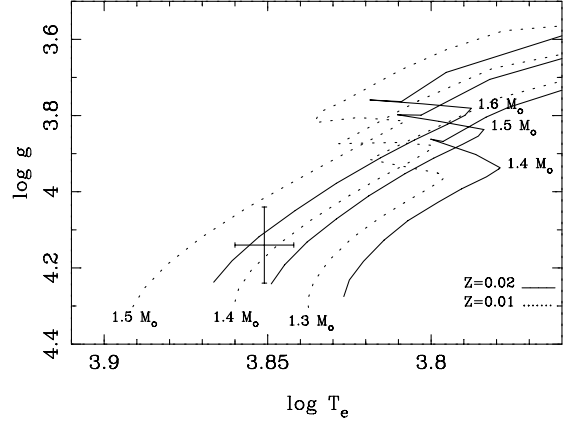


Fig. 4. Position of HD 239276 in the HR diagram with associated error bars and evolution tracks for $Z = 0.01$ (solid lines) (Claret & Giménez 1995) and $Z = 0.02$ (dotted lines) (Claret 1995).

δ Sct-type variables. If we accept a λ Boo nature for HD 239276, we can assume a mass of $M = 1.58 M_{\odot}$ and an age of 1.0 Gyr for this star by using the evolutionary tracks of Claret (1995) with $Z = 0.02$. Nevertheless, high-resolution spectra are necessary in order to clarify this point.

4. Pulsational content

The analysis of the pulsational content was carried out using the method described in Rodríguez et al. (1998) where Fourier and least-squares algorithms are combined in the same computation program package. When a new peak is found as significant in the periodograms, this together with all the previously determined frequencies are simultaneously optimized and extracted from the data together with the corresponding amplitudes and phases that minimize the residuals. Then, the method does not depend on successive prewhitenings of the data. The results thus obtained were checked using the new version of the computation package PERIOD (PERIOD04) (Lenz & Breger 2005). The two methods yield identical results.

This analysis stops when the new peaks suggested in the periodograms are not formally significant. Following Breger et al. (1993, 1999), a peak is considered as significant when the amplitude signal/noise (S/N) ratio is larger than 4.0 for independent frequencies or larger than 3.5 for harmonics or frequency combinations. The noise level was calculated by averaging the amplitudes of the residuals over 5 cd^{-1} boxes around the frequency under consideration.

Before analysing the periodograms of the variable, those corresponding to the comparison stars were checked in order to avoid misinterpretations in our results. Although C2 and C3 are placed beyond the cool border of the γ Dor-region, periodicities produced by binarity effects or spots might take place in them. On the other hand, the time distribution of the observations was very similar for the variable and check stars. Thus, the investigation of the C2–C1 and C2–C3 Fourier spectra is of special importance in the low frequency domain where the instrumental and/or atmospheric problems generally manifest themselves, producing spurious peaks. In this sense, simultaneous multicolour photometry plays an important role: the pulsational amplitudes and phases in different filters must follow defined rules which make it possible to distinguish intrinsic from spurious peaks. Finally, taking into account that the main comparison star C1 lies within the δ Sct limits, it is also very important to

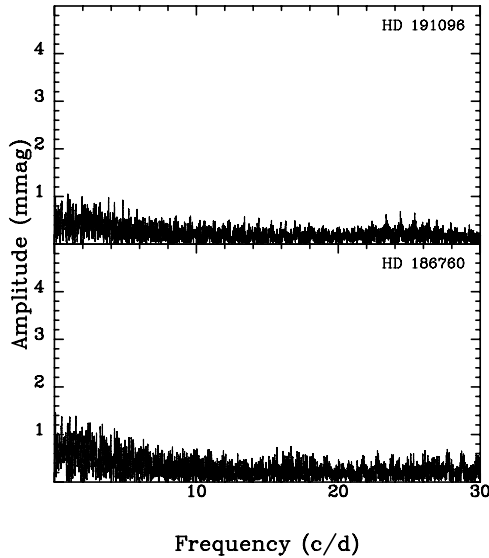


Fig. 5. Amplitude spectra of C2 = HD 191096 and C3 = HD 186760 in the b band.

verify the constancy of the C2–C1 and C3–C1 periodograms in the region of the high frequencies where δ Sct-type variability could occur.

In the present work, none such effects seem to be present. Only a very small increase in power is shown in the periodograms of the comparison stars, as seen in Fig. 5 for the b band, probably produced by nightly zero-point shifts. No periodicities are photometrically detected in the low region larger than about 1.4 mmag (or 0.6 mmag in the region beyond 10 cd^{-1}). These limits are lower than the internal error per single measurement collected for the variable (about 2.0 mmag in v and b). Hence, the limit in our investigation for the variable is defined by the significance level in the corresponding amplitude spectra. A peak can be considered as intrinsic to this star when it is found significant in its periodograms.

Although the main periodicities expected from the observed light curves of HD 239276 are typical of γ Dor-type variables, the possibility of short-period pulsations, typical of δ Sct-type stars, cannot be ruled out taking into account the location of this star in the H-R diagram. The discovery of new examples with both types of pulsations in the same star is, presently, a very exciting task. Thus, in order to check this possibility, the amplitude spectra were investigated in the full range of possible frequencies, but no significant peaks were found in the high frequency domain. In the region higher than 10 cd^{-1} , the periodograms always appear flat, resembling white noise similar to that shown in the right parts of Fig. 6.

For consistency in our results, the vby data were combined following the method described in Rodríguez et al. (2001). This way, the by data were transformed to simulate the v amplitudes and the measurements collected at each instant in filters v , b and y were averaged with weights according to their internal precision. Thus, a combined vby “filter” was built. In addition, the Johnson V data were also aligned. The results of this analysis are presented in Fig. 6 and Table 7 with three close frequencies found as significant around 2 cd^{-1} . Besides them, a fourth peak is detected at 1.56 cd^{-1} , but with $S/N = 3.8$, which is lower than the formal limit of 4.0. In fact, when the 4-frequency solution is applied to the four $uvby$ filters for the data collected at SNO, the S/N values are in all cases smaller than 3.0. Then, although there are some indications that favour the reliability of this peak,

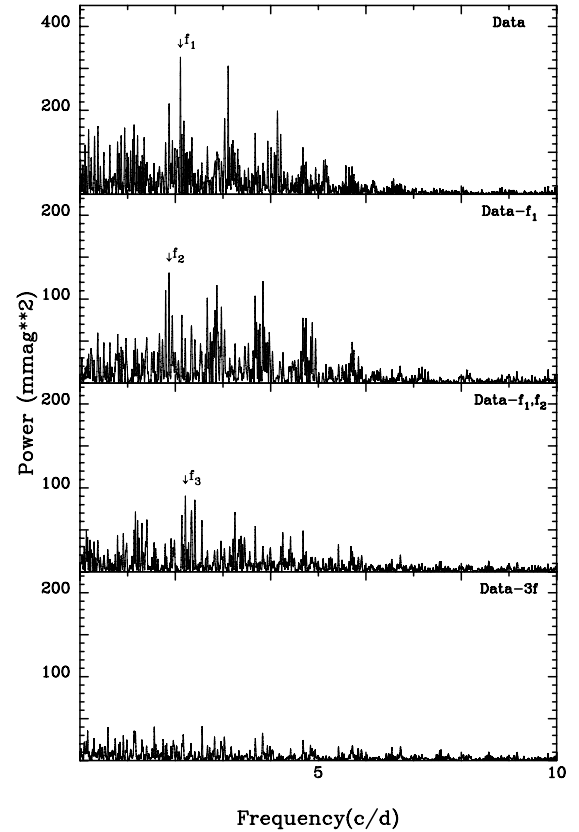


Fig. 6. Power spectra of HD 239276 in the combined vby band corresponding to the original data and residuals after removing different sets of simultaneously optimized peaks.

Table 7. Frequencies, amplitudes and amplitude signal/noise ratios obtained for the combined vby filter.

Frequency (cd^{-1})	Amplitude (mmag)	S/N
	± 0.71	
$f_1 = 2.1066$	18.98	9.5
4		
$f_2 = 1.8694$	17.15	8.6
5		
$f_3 = 2.2124$	11.64	5.8
7		

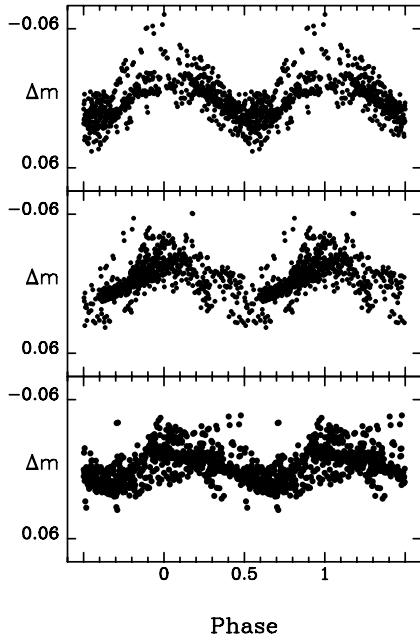
we will only consider the 3-frequency solution as definitive for our data set.

Nevertheless, the residuals of the 3-frequency solution ($\sigma = 11.4 \text{ mmag}$) are too large (much higher than expected). This is also shown in the bottom panel of Fig. 6. In particular, the power in the low frequency region is much higher than that at higher frequencies. This suggests that more periodicities, with smaller amplitudes, remain among the residuals, but our data set is not long enough to resolve them. Figure 7 shows the data phased at each of the three frequencies after prewhitening for the other two.

Table 8 shows the results when applying our 3-frequency solution to each of the four $uvby$ data. As seen, the residuals are much larger than expected. Moreover, the residuals decrease from filters v to b and y , that is, following the same sense of decreasing pulsational amplitudes. This confirms the fact that some frequencies are still present in the residual light curves. Table 9 lists the corresponding phase shifts and amplitude ratios, relative

Table 8. Results from the Fourier analysis applied to the four *uvby* filters.

Frequency (cd^{-1})	<i>u</i>			<i>v</i>			<i>b</i>			<i>y</i>		
	<i>A</i> (mmag)	φ (rad)	<i>S/N</i>									
	± 0.76			± 0.84			± 0.72			± 0.63		
$f_1 = 2.1066$	11.64	1.442	7.3	18.68	1.565	8.1	16.56	1.560	8.5	13.62	1.641	9.4
		58			40			38			41	
$f_2 = 1.8694$	10.90	1.645	6.8	16.27	1.533	7.1	14.82	1.586	7.6	11.67	1.631	8.0
		66			49			46			51	
$f_3 = 2.2124$	8.07	4.478	5.0	12.60	4.355	5.5	11.21	4.342	5.7	8.03	4.210	5.5
		87			61			59			72	
residuals (mmag)	10.5			11.5			9.8			8.6		

**Fig. 7.** Phase diagrams for $f_1 = 2.1066 \text{ cd}^{-1}$ (top), $f_2 = 1.8694 \text{ cd}^{-1}$ (middle) and $f_3 = 2.2124 \text{ cd}^{-1}$ (bottom). In each panel, the data have been whitened to remove the other two frequencies.

to the *y* filter, for the three main frequencies. The results are consistent, in all cases, with γ Dor-type pulsation (Rodríguez 2005).

5. Modal identification

5.1. Multicolour photometry

The theoretical monochromatic magnitude variation of a non-radial mode is given by:

$$\delta m_\lambda = -\frac{2.5}{\ln 10} \epsilon P_\ell^m(\cos i) b_{\ell\lambda} \times \left(-(\ell-1)(\ell+2) \cos(\sigma t) + f_T \cos(\sigma t + \psi_T) (\alpha_{T\lambda} + \beta_{T\lambda}) - f_g \cos(\sigma t) (\alpha_{g\lambda} + \beta_{g\lambda}) \right). \quad (1)$$

The meaning of the different terms and coefficients of this equation is given in Dupret et al. (2003). As this equation depends strongly on the degree ℓ of the mode, it can be identified by comparing the theoretical and observed amplitude ratios between different photometric passbands. This method has been applied to

Table 9. Observed phase shifts and amplitude ratios.

Frequency (cd^{-1})	<i>u</i> - <i>y</i> ($^\circ$)	<i>v</i> - <i>y</i> ($^\circ$)	<i>b</i> - <i>y</i> ($^\circ$)	<i>u</i> / <i>y</i>	<i>v</i> / <i>y</i>	<i>b</i> / <i>y</i>
$f_1 = 2.1066$	-11.4	-4.3	-4.6	0.85	1.37	1.22
	5.7	4.6	4.5	7	9	8
$f_2 = 1.8694$	0.8	-5.6	-2.6	0.93	1.39	1.27
	6.7	5.7	5.5	8	10	9
$f_3 = 2.2124$	15.3	8.3	7.6	1.00	1.57	1.40
	9.1	7.7	7.5	12	16	14

many types of pulsating stars. In particular, Dupret et al. (2005) applied it successfully to γ Dor stars, using for the first time in this frame non-adiabatic time-dependent convection models.

Two important coefficients of Eq. (1) are the normalized amplitude (f_T) and phase (ψ_T) of local effective temperature variation. These two quantities can only be theoretically determined by non-adiabatic models. Dupret et al. (2005) showed that time-dependent convection models (Grigahcène et al. 2005) must be used to reach a good agreement with observations.

5.1.1. Model independent mode identification

As a first step, we consider in this section f_T and ψ_T as free parameters and determine which values are required to get the best agreement between theory and observations. This will give us a model independent mode identification of the degree ℓ of the modes. In the next section, we will determine which theoretical models are able to reproduce these values.

In Fig. 8, we show the amplitude ratios obtained for different values of f_T . For the modes f_1 and f_2 , we see that good agreement with observations can only be obtained with $\ell = 1$ modes. The best values for f_T are $f_T \approx 0.15-0.2$ for f_1 and $f_T \approx 0.2-0.3$ for f_2 . $\psi_T \approx -35^\circ$ is required to get a good agreement with the observed phase differences. For the mode f_3 , the best agreement is found for an $\ell = 2$ mode with $f_T \approx 5$ but because of the large observational error bars, $\ell = 1$ cannot be completely discarded. As shown in Aerts et al. (2004) and Dupret et al. (2005), we see that very small values of f_T are required for γ Dor stars.

5.1.2. Time-dependent convection (TDC) study

In this section, we use stellar models computed with the Liege stellar evolution code CLES (Code Liégeois d'Évolution Stellaire) that uses: standard MLT for convection calculations; the OPAL opacities (Iglesias & Rogers 1996) completed at low temperatures with the opacities of

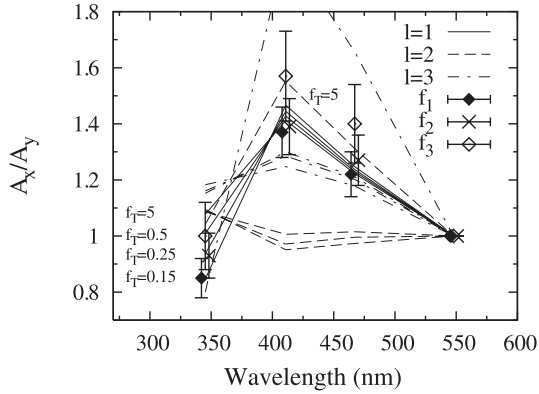


Fig. 8. Strömgren photometric amplitude ratios obtained for different values of f_T (0.15, 0.25, 0.5, 5), $\psi_T = -35^\circ$, $\log T_e = 3.85$, $\log g = 4.14$. The lines are the theoretical predictions for different l and the error bars represent the observations for the frequencies f_1 , f_2 and f_3 .

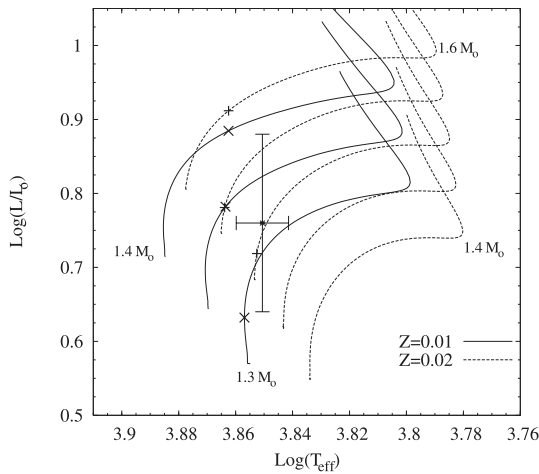


Fig. 9. Position of HD 239276 in the HR diagram with associated error bars and evolution tracks for $Z = 0.01$ (solid lines) and $Z = 0.02$ (dotted lines) using the CLES code. Some of our best models for $Z = 0.01$ (\times) and $Z = 0.02$ ($+$) are also shown.

Alexander & Ferguson (1994); the CEFF equation of state (Christensen-Dalsgaard & Däppen 1992); and the atmosphere models of Kurucz (1998) as boundary conditions. Non-adiabatic computations using TDC models (Grigahcène et al. 2005) enable us to determine the stability of the modes and the theoretical values of f_T and ψ_T for different models. These values can be used to determine the photometric amplitude ratios and compare them with observations.

We begin with the results of our stability analysis. The frequencies of HD 239276 are relatively high compared to those of typical γ Dor stars. For all the theoretical TDC models considered in this study, $l = 1$ modes are near the limit between stability and instability for $f \approx 2$ c/d. For $l \geq 2$, the modes are always predicted to be unstable in the observed range.

We consider now the values found for f_T and the corresponding amplitude ratios. In Fig. 9, we give the location of HD 239276 in the HR diagram, as deduced from Table 6, that is, $T_e = 7090$ K and $\log L/L_\odot = 0.76$. As expected, the new models using the CLES code provide slightly different masses to those derived in Sect. 3 as consequence of the existing differences in some ingredients used. In particular, in the case of HD 239276, the new masses are about 4% and 7% smaller than those derived from Claret's models for $Z = 0.020$ and $Z = 0.010$,

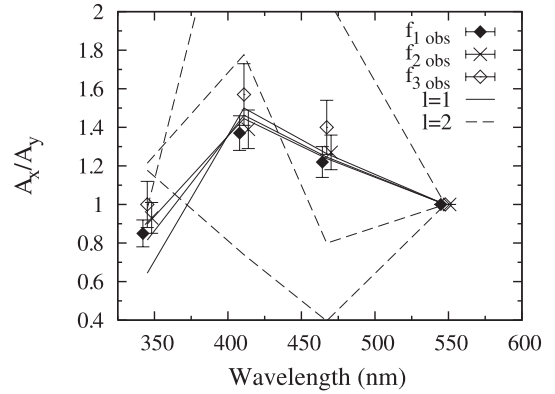


Fig. 10. Strömgren photometric amplitude ratios obtained with our TDC treatment, for a model with $M = 1.5 M_\odot$ and $Z = 0.02$ in the centre of the photometric error box ($\log T_e = 3.8508$). The lines are the theoretical predictions for $l = 1$ (solid) and $l = 2$ (dashed) modes with frequencies closest to the observed ones. The error bars represent the observations for the frequencies f_1 , f_2 and f_3 .

respectively. We begin by considering the results obtained for a model in the centre of this photometric error box with $Z = 0.02$ ($M = 1.5 M_\odot$, $\log T_e = 3.8508$). Figure 10 shows the comparison between the theoretical and observed amplitude ratios for this model, for $l = 1$ and $l = 2$ modes. The $l = 3$ modes are not given as the associated amplitude ratios completely disagree with observations. We see that the agreement is very good for f_1 and f_2 , identified as $l = 1$ modes. It is more difficult to obtain agreement for f_3 (with larger error bars).

As a second step, we consider models with different masses, metallicities and ages and determine those giving the required values for f_T . All these models are with mixing-length parameter $\alpha = 2$. In Table 10, the values of f_T obtained for these models are listed. The values found for ψ_T are around $[-60^\circ, -15^\circ]$. More precisely, we give the values of f_T obtained for the $l = 1$ g-mode with a frequency closest to that of f_1 , for the $l = 1$ g-mode with frequency closest to that of f_2 and for the $l = 2$ mode with frequency closest to that of f_3 . We get the required values $f_T \approx 0.15$ – 0.2 for f_1 and $f_T \approx 0.2$ – 0.3 for f_2 for a $M = 1.5 M_\odot$, $Z = 0.02$ model with the photometrically determined effective temperature and luminosity (Fig. 10).

We consider this model (boldfaced in Table 10) as our best one. It is also possible to obtain the required values of f_T with other models. These models are represented by $+$ and \times in Fig. 9 and we see that they are out of the photometric error box. As an example, the deduced amplitude ratios obtained for one of our best models with $Z = 0.01$ are plotted in Fig. 11. However, none of these best models gives the required high value of f_T for the mode f_3 ($l = 2$); higher mass would be required as shown by the $1.6 M_\odot$, $\log T_e = 3.8727$ result of Table 10. For these best models, the $l = 1$ theoretical predictions agree with observations better than the $l = 2$ ones for f_3 , but discrepancy is still present and we do not obtain conclusive results for this mode.

As conclusion, in our photometric mode identification using TDC models, f_1 and f_2 are identified as $l = 1$ modes. No conclusive mode identification is found for f_3 . The differences found between our $Z = 0.01$ and $Z = 0.02$ theoretical results are small and do not allow us to discriminate between a λ Bootis and a submetallic nature for this star.

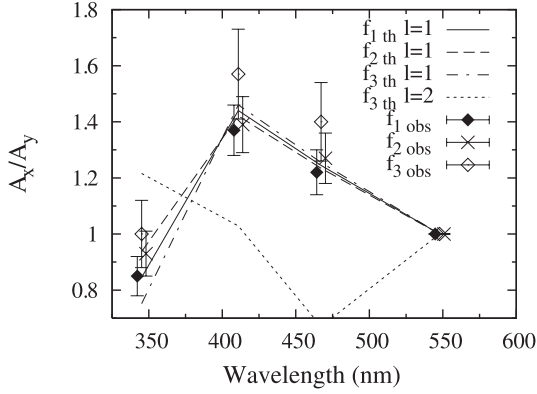


Fig. 11. Strömgren photometric amplitude ratios obtained with our TDC treatment, model with $M = 1.3 M_{\odot}$, $Z = 0.01$, $\log T_e = 3.8569$, $\alpha = 2$. The lines are the theoretical predictions (e.g. f_1 th $l = 1$ means theoretical result for the $l = 1$ mode with frequency closest to f_1). The error bars represent the observations for the frequencies f_1 , f_2 and f_3 .

Table 10. Theoretical values of f_T .

M (M_{\odot})	Z	$\log T_e$	$\log g$	f_T		
				f_1 $\ell = 1$	f_2 $\ell = 1$	f_3 $\ell = 2$
1.5	0.02	3.8526	4.26	0.21	0.29	0.86
		3.8508	4.22	0.16	0.22	0.79
		3.8437	4.15	0.07	0.12	0.55
1.55	0.02	3.8638	4.26	0.19	0.38	0.98
		3.8578	4.18	0.06	0.17	0.58
		3.8465	4.10	0.02	0.07	0.41
1.6	0.02	3.8727	4.22	1.72	2.89	6.28
		3.8625	4.13	0.31	0.60	1.48
		3.8552	4.08	0.06	0.08	0.39
1.3	0.01	3.8569	0.632	0.19	0.32	0.82
		3.8524	0.708	0.11	0.21	0.65
		3.8441	0.748	0.02	0.08	0.45
1.35	0.01	3.8636	0.782	0.18	0.30	0.74
		3.8580	0.804	0.05	0.12	0.39
		3.8472	0.830	0.04	0.03	0.34
1.4	0.01	3.8723	0.861	1.38	2.28	5.66
		3.8625	0.884	0.21	0.40	1.14
		3.8546	0.898	0.07	0.07	0.24

5.2. The frequency ratio method

Following Moya et al. (2005) the frequency ratio method (FRM) was applied to HD 239276 in order to obtain information on: 1) possible identification of the radial order n and degree l of the modes corresponding to the observed frequencies and 2) an estimate of the integral of the buoyancy frequency (Brunt-Väisälä) weighted over the stellar radius along the radiative zone (I). We follow the same scheme adopted in Rodríguez et al. (2006) for the γ Dor star HD 218427, and assume that all the excited modes correspond to the same azimuthal order $m = 0$.

From the multicolour photometry results given in the previous section, a possible mode degree l identification is provided for each observed mode. This allows us to apply the FRM without assuming the hypothesis of equal l , that is, using the generalized form given by Eq. (6) of Moya et al. (2005). In particular, multicolour photometry analysis predicts f_1 and f_2 identified as

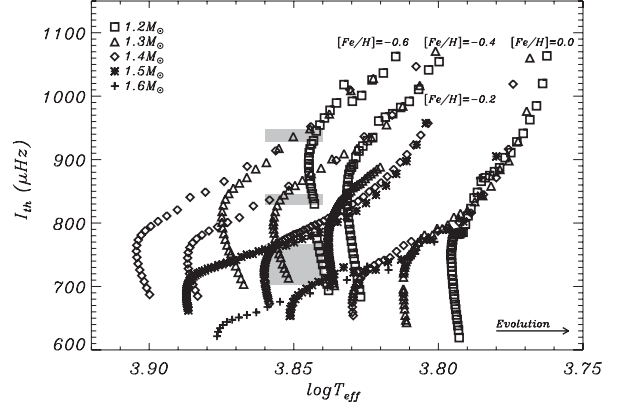


Fig. 12. Theoretical Brunt-Väisälä frequency integral as a function of the effective temperature for representative models with masses in the range of $M = 1.2$ – $1.6 M_{\odot}$ and different metallicities $[Me/H] = 0.0$, -0.2 , -0.4 , and -0.6 . Shaded areas represent uncertainty (I_{obs} , T_{eff}) boxes for the solutions given in Table 11.

Table 11. List of possible (n, l, I_{obs}) identifications provided by the FRM applied to the observed frequencies of HD 239276. The first three columns represent the resulting (n, l) identifications. The last column corresponds to the *observed* Brunt-Väisälä integral.

(n_2, ℓ_2)	(n_1, ℓ_1)	(n_3, ℓ_3)	I_{obs}
(25, 2)	(22, 2)	(21, 2)	703.60
(26, 2)	(23, 2)	(22, 2)	734.87
(27, 2)	(24, 2)	(23, 2)	766.14
(17, 1)	(15, 1)	(25, 2)	837.46
(19, 1)	(17, 1)	(16, 1)	938.57

$\ell = 1$ modes and f_3 as $\ell = 1, 2$ modes. We can thus apply the FRM searching for natural number sets fulfilling

$$\frac{\sigma_{n_1, \ell_1} \sqrt{\ell_2(\ell_2 + 1)}}{\sigma_{n_2, \ell_2} \sqrt{\ell_1(\ell_1 + 1)}} \approx \frac{n_2 + 1/2}{n_1 + 1/2}. \quad (2)$$

Since no information is provided concerning the rotational velocity of this object, and the observed frequencies are close to the limit of validity of the asymptotic regime, intrinsic errors larger than those used in Moya et al. (2005) must be considered when applying the FRM (see Suárez et al. 2005). In the present case an error bar of $\pm 1.2 \times 10^{-2}$ is used when applying Eq. (2).

In Table 11, the FRM solutions are listed. For each possible solution, an estimate of the observed Brunt-Väisälä integral I_{obs} is also provided. This new observable allows us to obtain a model constraint by placing it in a $I_{\text{th}} - \log T_e$ diagram as described in Moya et al. (2005), where I_{th} represents the theoretical Brunt-Väisälä integral calculated from equilibrium models. In Fig. 12, such a diagram is depicted for the solutions given in Table 11 with the corresponding error boxes. Notice that the only solution for which the observed integrals lies close to the solar metallicity tracks region is the one assuming all the modes having $\ell = 2$, which contradicts the multicolour analysis results. When considering f_3 as a $\ell = 2$ mode (f_1 and f_2 as $\ell = 1$ modes), the solutions are compatible with the observed metallicity ($[Me/H] = -0.4$). For f_3 as $\ell = 1$ mode (f_1 and f_2 as $\ell = 2$ modes), no solutions are found. For the case of the three modes are identified as $\ell = 1$ modes, the solutions are compatible with models around $[Me/H] = -0.6$ dex.

Therefore, for three of four possible ℓ combinations studied, the FRM provides solutions compatible with the observed metallicity ± 0.2 dex. However, there is no evidence that ensures

the discrimination between these three solutions. Nevertheless, the case of the three observed frequencies being identified as $\ell = 2$ modes is in contradiction with the results from our multicolour photometry analysis given in the previous section. Then, the results obtained by both mode discrimination methods agree for only the two solutions with the lowest metallicities. This suggests a metal-deficient abundance in HD 239276.

However, a more detailed study of this star is needed in order to confirm our results. As discussed in previous sections HD 239276 is a suspected λ Boo-type star and therefore its metallic composition could be underestimated. The metal particularities of λ Boo-type stars may induce changes in the stellar structure, for instance by means of some microscopic diffusion, which may change the results in the application of our identification modes. It is interesting to note that similar discordant results are also found when applying the method to the confirmed λ Boo star HR 8799 (Suárez et al. 2006).

6. Conclusions

In this work, we present the results of two-site photometric observations carried out during the autumn of 2001 from China and Spain in order to confirm and study the variability of the star HD 239276. The observations collected in Spain consisted of simultaneous *uvby* measurements together with data obtained in the H_{β} -Crawford system, while those obtained in China consisted of Johnson *V* photometry.

The analysis of its colour indices places this star in the γ Dor instability region. This is confirmed by the spectral type A9V derived from two low-dispersion spectra obtained in this work. This is much later than that of A3 listed in the Simbad database (Simbad 2006), but agrees with the long-period variability (about 0.5 days) observed in this star.

The physical parameters of HD 239276 were determined using the *uvby* β indices derived in this work together with the most suitable Strömngren photometric calibrations available in the literature, including atmospheres and stellar evolution models. The results establish this star as a γ Dor-type pulsator with deficiency in metallicity, similar to other already known γ Dor stars, such as HR 8799 (Gray & Kaye 1999) and HD 218427 (Rodríguez et al. 2006). The possibility of a λ Boo nature is discussed. In such a case, the metallicity content of HD 239276 could be underestimated. Nevertheless, high-resolution spectra are necessary to clarify this point.

The frequency analysis of our data shows the existence of at least three pulsation frequencies, and some more periodicities probably remain among the residuals. New observations from a further coordinated multisite photometric campaign will be of crucial importance to study the full pulsational behaviour of this variable. Nevertheless, the already derived phase shifts and amplitude ratios between different filters for the three main periodicities are in all cases consistent with γ Dor-type pulsation.

In order to perform an identification of the spherical degree l of the excited modes, two recently developed methods suitable for γ Dor-type pulsators have been used: 1) that based on the observed phase shifts and amplitude ratios among different filters

in multicolour photometry using a non-adiabatic time-dependent convection (TDC) treatment (Dupret et al. 2005; Grigahcène et al. 2005) and 2) the frequency-ratio method (FRM) (Moya et al. 2005) based on the observed frequency ratios which is particularly useful when at least three oscillation frequencies are present in the light curves. When using the former method, a very good agreement is obtained between the theoretical and observed amplitude ratios and the two main modes are identified as $l = 1$ modes. This is compatible with the results derived using the FRM. Moreover, the joint results suggest low metallicity for HD 239276, but a λ Boo nature is not ruled out.

Acknowledgements. This research was partially supported by the Junta de Andalucía and the Dirección General de Investigación (DGI) under projects AYA2003-4651 and ESP2004-03855-C03-01. J.C.S. acknowledges the financial support of the European Marie Curie action MERG-CT-2004-513610 and the Spanish Consejería de Innovación, Ciencia y Empresa, from the Junta de Andalucía local government. M.A.D. acknowledges financial support from the CNRS. This research has made use of the Simbad database, operated at CDS, Strasbourg, France.

References

- Aerts, C., Cuypers, J., De Cat, P., et al. 2004, *A&A*, 415, 1079
 Alexander, D. R., & Ferguson, J. W. 1994, *ApJ*, 437, 879
 Breger, M., Stich, J., Garrido, R., et al. 1993, *A&A*, 271, 482
 Breger, M., Handler, G., Garrido, R., et al. 1999, *A&A*, 349, 225
 Claret, A. 1995, *A&AS*, 109, 441
 Claret, A., & Giménez, A. 1995, *A&AS*, 114, 549
 Christensen-Dalsgaard, J., & Däppen, W. 1992, *A&AR*, 4, 267
 Dupret, M.-A., De Ridder, J., De Cat, P., et al. 2003, *A&A*, 398, 677
 Dupret, M.-A., Grigahcène, A., Garrido, R., et al. 2005, *MNRAS*, 360, 1143
 Gray, R. O. 1988, *AJ*, 95, 220
 Gray, R. O., & Corbally, C. J. 1993, *AJ*, 106, 632
 Gray, R. O., & Garrison, R. F. 1989, *ApJS*, 69, 301
 Gray, R. O., & Kaye, A. B. 1999, *AJ*, 118, 2993
 Grigahcène, A., Dupret, M.-A., Gabriel, M., et al. 2005, *A&A*, 434, 1055
 Handler, G. 1999, *MNRAS*, 309, L19
 Handler, G., & Shobbrook, R. R. 2002, *MNRAS*, 333, 251
 Henry, G. W., Fekel, F. C., & Henry, S. M. 2005, *AJ*, 129, 2815
 Iglesias, C. A., & Rogers, F. J. 1996, *ApJ*, 464, 943
 Kurucz, R. L. 1998, <http://cfaku5.harvard.edu/grids.html>
 Krisciunas, K. 1993, *Comments on Astrophysics*, 17, 4
 Lenz, P., & Breger, M. 2005, *CoAst*, 146, 5
 Moya, A., Suárez, J. C., Amado, P. J., Martín-Ruiz, S., & Garrido, R. 2005, *A&A*, 432, 189
 Nather, R. E., Winget, D. E., Clemens, J. C., et al. 1990, *ApJ*, 361, 309
 Olsen, E. H. 1996, private communication
 Rodríguez, E. 2005, *PASPC*, 333, 165
 Rodríguez, E., & Breger, M. 2001, *A&A*, 366, 178
 Rodríguez, E., & Zerbi, F. 1995, *Inf. Bull. Var. Stars*, 4170
 Rodríguez, E., Rolland, A., & López de Coca, P. 1993, *A&AS*, 100, 571
 Rodríguez, E., González-Bedolla, S. F., Rolland, A., Costa, V., & López de Coca, P. 1997, *A&A*, 324, 959
 Rodríguez, E., Rolland, A., López-González, M. J., & Costa, V. 1998, *A&A*, 338, 905
 Rodríguez, E., López-González, M. J., Rolland, A., Costa, V., & González-Bedolla, S. F. 2001, *A&A*, 376, 489
 Rodríguez, E., Amado, P. J., Suárez, J. C., et al. 2006, *A&A*, 450, 715
 Shuster, W. J., & Nissen, P. E. 1986, *Inf. Bull. Var. Stars*, 2943
 Simbad 2006, Simbad Database, CDS, Strasbourg, France
 Suárez, J. C., Moya, A., Martín-Ruiz, S., et al. 2005, *A&A*, 443, 271
 Suárez, J. C., et al. 2006, in preparation
 Zerbi, F., Rodríguez, E., Garrido, R., et al. 1999, *MNRAS*, 303, 275